

State-selective charge transfer in slow collisions of C^{4+} with H and H_2

R. Hoekstra,* J. P. M. Beijers, A. R. Schlattmann, and R. Morgenstern
Kernfysisch Versneller Instituut, Zernikelaan 25, 9747 AA Groningen, The Netherlands

F. J. de Heer

FOM-Institute for Atomic and Molecular Physics, P.O. Box 41883, 1009 DB Amsterdam, The Netherlands

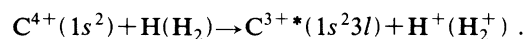
(Received 28 November 1989)

Absolute state-selective electron-capture cross sections for charge transfer into the $3l$ state of C^{3+} in collisions of C^{4+} on H and H_2 have been measured in the impact energy range of 0.05–1.33 keV/amu. The low-energy beams have been produced by retarding a 1.33-keV/amu C^{4+} beam (16 keV) by means of a five-element electrostatic lens system. The experimental results are compared with calculations based on molecular and atomic basis-set expansions. It turns out that especially for energies below 200 eV/amu there are considerable differences between experiment and theory both in relative and absolute $3l$ state-selective cross sections.

I. INTRODUCTION

Charge transfer in collisions of highly charged ions with neutral gas atoms, especially atomic hydrogen, has recently attracted much attention (see, e.g., the reviews by Janev and Winter¹ and Gilbody²). This interest stems not only from fundamental aspects but also from the importance of electron-capture processes in astrophysics³ and plasma physics.^{4,5} In the low-energy region ($E \ll 1$ keV/amu) much theoretical work has been done on (quasi-) one-electron systems. Experimental results in this low-energy region are still scarce, which is mainly due to difficulties in producing both intense slow highly charged ion beams and dense atomic hydrogen targets. For impact energies well below 1 keV/amu total charge-transfer cross sections for differently charged C, N, and O ions have been measured by Phaneuf *et al.*,⁶ Havener *et al.*⁷ and Huq *et al.*⁸ Comparing the experimental total charge-transfer cross sections with theoretical predictions it is found that there are often discrepancies, see, e.g., Gargaud and McCarroll⁹ (O^{4+}), Havener *et al.*⁷ (O^{5+}), and Gargaud *et al.*¹⁰ (C^{4+}). To find the reason for the disagreements and to obtain more insight in low-energy electron-capture processes, state-selective cross sections are needed.

To address this need we have installed an electrostatic lens system to retard the primary ion beams, which allows us to extend our photon-emission measurements (see, e.g., Dijkkamp *et al.*¹¹ and Hoekstra *et al.*¹²) down to lower energies. After the successful feasibility study on the system He^{2+} -H (Hoekstra *et al.*¹³), we have now performed an extensive series of measurements on C^{4+} colliding with atomic and molecular hydrogen. The capture processes that have been studied by means of photon-emission spectroscopy are



The C^{4+} -H system is one of the benchmark systems of theoretical work.^{10,14–17} Comparing the theoretical and

experimental⁶ total electron-capture cross sections it is found that there are considerable differences, especially in the energy range of 100 to 300 eV/amu. In that energy range the calculations based on molecular-state expansions (Olson *et al.*,¹⁴ Hanssen *et al.*,¹⁵ and Gargaud *et al.*¹⁰) are in good agreement with each other, nevertheless they overestimate the experimental total electron-capture cross sections by almost a factor of 2. The atomic-orbital calculations of Fritsch and Lin¹⁶ are in better agreement with the experiments. Amazingly enough the best agreement is found for the “small basis set” molecular-orbital calculations of Gargaud and McCarroll,¹⁷ although these calculations include only radial couplings, whereas their most recent work¹⁰ includes both radial and rotational couplings. A more stringent test of the status of the calculations can be provided by state-selective charge-transfer cross sections, since inclusion of rotational coupling has different effects on the dominantly populated $3l$ states, namely whereas the $3s$ capture cross section decreases, the $3p$ and $3d$ cross sections increase.^{10,17} Before discussing our state-selective cross sections for collisions on atomic and molecular hydrogen we will first describe briefly the general features of the experiment, and in more detail the beam-retardation technique.

II. EXPERIMENT

The C^{4+} ions have been produced by the electron cyclotron resonance (ECR) ion source of the MINIMAFIOS-type¹⁸ installed at the Kernfysisch Versneller Instituut in Groningen.¹⁹ The electrical ion beam current in the collision region was some 250 nA at an extraction voltage at 4 kV. This low extraction voltage is a compromise between a decreasing output of the ECR ion source with decreasing extraction voltage and the maximum voltage that can be held by the deceleration lens. In the experimental setup, the main features of which are schematically shown in Fig. 1, the 16 keV C^{4+} ions are retarded to the desired energy by a five-element

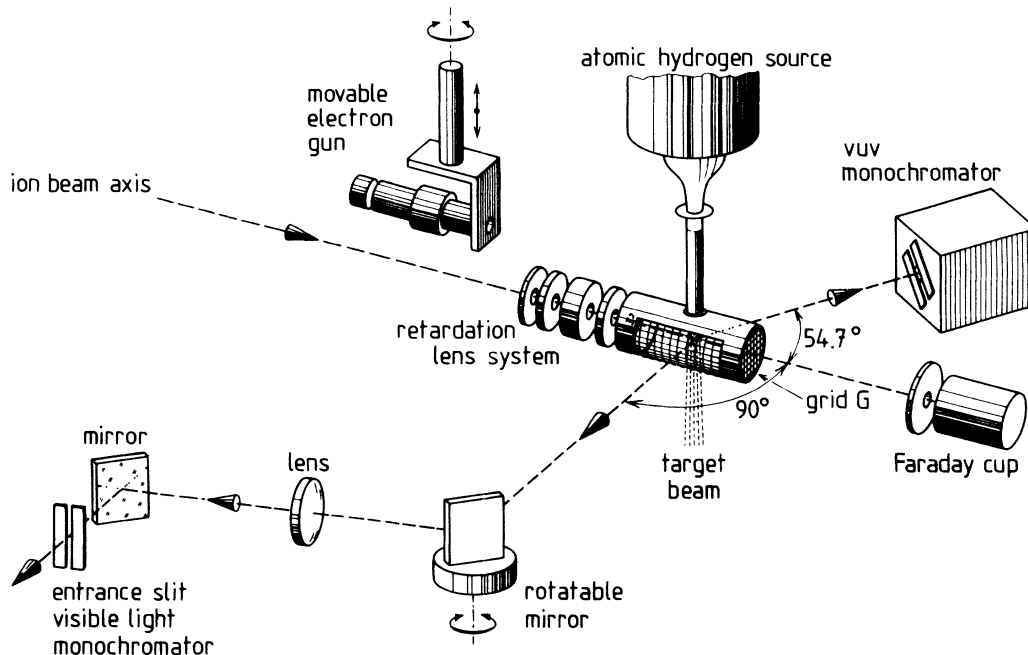


FIG. 1. Schematic view of the setup.

lens system of the Menzinger type.²⁰ Both the first and the last elements have a beam-collimating diaphragm of 3 mm. The last element is extended by a copper cylinder with an inner diameter of 10 mm which encloses the collision region (see Fig. 1). Hence the potential difference between the last element and the ECR ion source defines the kinetic energy of the C^{4+} beam at the crossing with the target beam. To cancel ripples, drift and instabilities in the ECR voltage the (high-) voltage power supplies of the lens elements are connected in series with the power supply of the ECR ion source. It should be noted that in this way the plasma potential of the ECR ion source plasma is not canceled. Since during the period of our experiments plasma potentials between 8 and 16 V have been observed²¹ (minimum and maximum values ever measured are 7 and 20 V,²² respectively), we have included a plasma potential of 12 V in all our measurements. At the lowest energy reached, 48 eV/amu (144 V), this plasma potential of 12 V accounts for almost 10% of the kinetic energy of the C^{4+} beam. The profiles of the retarded ion beams have been calculated with the program LENS.²² The divergence of the primary beam is 12 mrad. Figure 2 shows (schematically) the beam profiles, with and without grid G for the case of decelerating a 16 keV C^{4+} beam down to 1.6 keV (133 eV/amu).

With grid G in place it turns out that below approximately 180 eV/amu (540 V) it is no longer possible to perform reliable measurements. This is due to the following facts. (i) A fraction of the ion beam falls on the guard ring of the Faraday cup (Fig. 2), which hampers an accurate measurement of the total beam current, since highly charged ions like C^{4+} produce a considerable number of secondary electrons.^{22,23} In this respect it should be not-

ed that in reality the Faraday cup is more than twice as deep as shown in Fig. 2 and besides that, it is biased by 60 V, which prevents the secondary electrons to escape from the cup. (ii) The ion beams become unstable whenever a

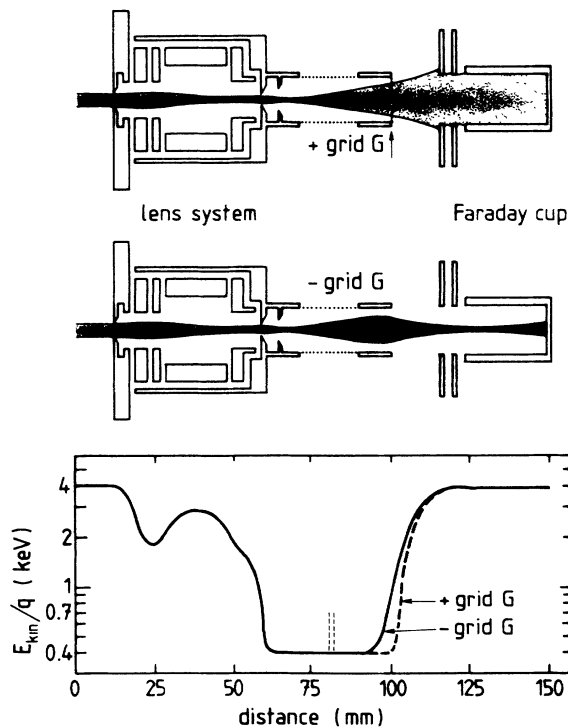


FIG. 2. Beam profiles and kinetic energies—with (+) and without (–) grid G —for retarding the ion beam of 4 keV down to 0.4 keV. The range between the thin vertical dashed lines is the region seen by the spectrometers.

fraction ($> 5\%$) of the beam falls on the guard ring. In this case the scatter in the results can be 50%, hence much larger than the error in the current measurement. These instabilities might be due to small sparks and discharges initiated by the electrons ejected from the guard ring and of course by the electrons produced due to collisions with grid *G*, which has a transmission of 87%.

In the case without grid *G* the ion beam is fully collected in the Faraday cup (Fig. 2). Furthermore, there is the advantage that the beam does not interact with the grid *G*. The only problem that may arise is that the spread of the electrical field into the cylinder may still be of importance in the interaction region. From the kinetic energy diagram in Fig. 2 the penetration of the field into the cylinder can clearly be seen to be still negligible at the interaction region. Our calculations showed that in all cases the influence is less than 0.1 V. So below 200 eV/amu we can only work without grid, whereas above 200 eV/amu both methods can be and have been used to produce the retarded beams.

The decelerated beams cross a pure H_2 or a mixed $H-H_2$ target beam. In the latter case H_2 was partly dissociated by means of Slevin-type radio-frequency source.²⁴ The absolute density profiles of the atomic and molecular components of the beam were determined by observation of electron-impact-induced atomic (Balmer β) and molecular radiation. The radiation passing through the grid in the copper cylinder (see Fig. 1) was observed with a monochromator for visible light (300–600 nm) equipped with an imaging lens system which enabled the measurement of the density profiles along the beam axis. In this way (described in detail by Čirič *et al.*²⁵) we found an effective fraction of atomic hydrogen of 55%. The photon emission resulting from the decay of the $C^{3+}(3l)$ states was observed with a grazing incidence vacuum spectrometer for the vuv (10–80 nm), equipped with a position sensitive microchannel plate detector, which enables simultaneous detection of lines within ranges of about 20 nm. This spectrometer is positioned under the magic angle of 54.7° with respect to the ion beam and it is tilted by 45° , since under these angles influences of polarization effects cancel.^{26,27} The wavelength-dependent sensitivity of the spectrometers was determined absolutely by various electron- and ion-impact processes with known cross sections (see, e.g., Kadota *et al.*²⁸ and Dijkamp *et al.*¹¹). With the setup described above the following emission lines of C^{3+} have been measured: $3s \rightarrow 2p$ (42.0 nm), $3p \rightarrow 2s$ (31.2 nm), and $3d \rightarrow 2p$ (38.4 nm). For illustration Fig. 3 shows a spectrum for C^{4+} colliding with a mixed $H-H_2$ target. The areas of the various peaks are used to measure the intensities of the corresponding lines.

III. EXPERIMENTAL RESULTS

The experimental results are given in Tables I and II and shown in Figs. 4(a)–4(d) and 5(a)–5(d). The relative errors represent the quadratic sums of the statistical errors at 90% confidence level and target density uncertainties. The latter ones are due to possible fluctuations in

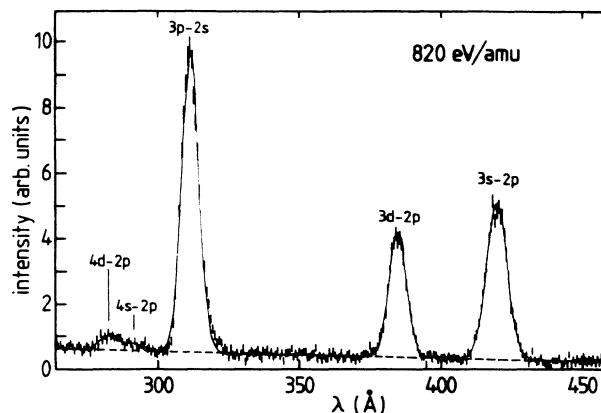


FIG. 3. Typical photon-emission spectrum for the case of C^{4+} colliding on a mixed $H-H_2$ target.

the target pressure, the dissociation degree, and the overlap of the ion and target beams. The stability of the dissociation degree of the atomic-molecular hydrogen target was checked before and after each C^{4+} measurement by measuring the $He II(2p \rightarrow 1s)$ line emission resulting from collisions with a 3 keV/amu He^{2+} beam. (Because the ECR ion source runs on a CO-He gas mixture and because the 3 keV/amu He^{2+} and 1.33 keV/amu C^{4+} beams have the same magnetic rigidity it is possible—beam transport through magnetic focusing and bending elements¹⁹—to change primary beams by just changing the extraction voltage of the ECR ion source.) Since the $He II(2p \rightarrow 1s)$ line emission cross section for collisions with atomic hydrogen is more than five times larger than with molecular hydrogen^{13,29} The intensity of this emission line is an accurate indicator of the dissociation degree. The target density was found to be extremely stable, respectively, within 1.5% and 3% for molecular and atomic hydrogen. The main contribution to the uncertainty in the effective target density is due to changes in the overlap of the ion and target beams. We have estimated this error to be 5% for energies above 250 eV/amu, 10% for energies between 150 and 250 eV/amu and 15% for energies below 150 eV/amu. To obtain these errors we have performed the following measurements: (i) measurements at different impact energies of line-emission ratios for collisions on a static and on a beam target of molecular hydrogen (the atomic hydrogen beam has the same full width half maximum as the molecular hydrogen beam²⁵), and (ii) measurements of the $C IV$ line emission for different voltages on the first four lens elements (see Fig. 2). Changing the lens voltages shifts the focus and hence alters the diameter of the ion beam at the crossing with the target beam. Besides these measurements we have performed beam-profile calculations. At the lowest energies it was found that at the crossing with the target beam the ion beam diameter can be changed between 3.7 and 5.0 mm. However, the effect on the effective target pressure is still relatively small since the full width half maximum of the target beam is ~ 7 mm.

TABLE I. State-selective [$\sigma(3l)$] and total (σ_t) electron-capture cross sections and relative errors, $\Delta\sigma$ for C^{4+} colliding with H in 10^{-16} cm².

E (eV/amu)	$\sigma(3s)$	$\Delta\sigma(3s)$	$\sigma(3p)$	$\Delta\sigma(3p)$	$\sigma(3d)$	$\Delta\sigma(3d)$	σ_t	$\Delta\sigma_t$
1333	12.5	2.0	12.7	1.8	8.0	0.8	33.2	3.5
1050	11.5	2.0	13.1	2.0	8.6	1.0	33.2	3.7
820	11.8	2.0	17.3	2.5	9.6	1.3	38.7	4.7
700	9.9	2.0	17.5	2.2	10.4	1.5	37.8	4.5
583	9.1	2.0	16.1	2.2	7.7	1.5	32.9	4.3
520	11.7	2.4	20.9	3.1	9.9	1.4	42.5	6.0
500	8.2	2.0	22.3	3.2	9.2	1.4	39.7	5.5
467	12.5	3.5	24.1	3.4	10.0	1.5	46.6	6.7
400	6.6	2.5	26.4	3.7	8.9	1.5	41.9	5.0
350	8.2	2.5	24.6	3.4	8.2	1.4	41.0	5.0
300	6.0	2.0	30.6	5.0	7.5	1.2	44.1	5.5
250	6.0	2.2	23.5	4.0	5.4	1.1	34.7	4.5
233	4.6	2.0	29.8	5.0	5.8	1.2	40.7	5.0
200	4.1	1.5	25.0	4.0	3.4	0.7	32.5	4.5
160	1.7	1.0	24.2	4.0	3.0	0.7	28.9	4.3
130	1.2	0.9	22.2	3.7	1.3	0.4	24.7	4.2
100	<<1.0		24.0	4.0	1.1	0.4	25.1	4.3
80	<<1.0		24.1	4.1	1.1	0.4	25.2	4.5
60	<<1.0		26.7	4.2	1.3	0.4	28.0	5.0
48	<<1.0		26.9	4.5	0.7	0.4	27.6	5.0
$\Delta\sigma_{\text{absolute}}$		22%		17%		20%		19%

One final contribution to the relative errors has still to be discussed, namely the influence of cascades from the $n=4$ states on the $3l$ state populations. All lifetimes involved are so short that complete cascading occurs within the viewing range of the monochromator. Dijkkamp *et al.*¹¹ have shown that at somewhat higher

energies (1–7 keV/amu) the $4l$ capture cross sections are more than one order of magnitude smaller than the $3l$ capture cross sections and furthermore that they decrease with decreasing energy. Notwithstanding all that, we kept track of the populations of $4l$ states by recording the $4l \rightarrow 2l'$ ($l=s,p,d$) transitions. These transitions, which

TABLE II. State selective [$\sigma(3l)$] and total (σ_t) electron capture cross sections and relative errors, $\Delta\sigma$ for C^{4+} colliding with H₂ in 10^{-16} cm².

E (eV/amu)	$\sigma(3s)$	$\Delta\sigma(3s)$	$\sigma(3p)$	$\Delta\sigma(3p)$	$\sigma(3d)$	$\Delta\sigma(3d)$	σ_t	$\Delta\sigma_t$
1333	14.7	1.5	6.7	0.7	4.5	0.5	25.9	2.6
1050	15.5	1.7	6.8	0.7	4.2	0.5	26.5	2.6
820	17.4	1.9	8.2	0.9	4.9	0.6	30.5	3.1
700	17.5	1.8	8.4	1.0	4.7	0.6	30.6	3.3
583	19.4	2.5	8.9	1.2	4.3	0.6	32.6	3.3
520	22.5	2.8	11.4	1.5	4.8	0.6	38.7	4.0
500	19.0	2.5	10.1	1.5	4.7	0.6	33.8	3.6
467	22.0	2.8	12.4	1.8	5.2	0.7	39.1	4.1
400	18.7	2.3	11.3	1.8	4.2	0.6	34.2	3.6
350	21.0	2.5	13.6	1.8	4.3	0.6	38.9	4.0
300	20.3	2.5	14.1	2.0	4.0	0.5	38.4	4.0
250	20.6	2.6	16.0	2.3	3.5	0.5	40.1	4.6
233	20.6	3.0	15.5	2.5	3.3	0.5	39.4	4.1
200	18.2	2.8	17.3	2.8	2.8	0.4	38.3	4.1
160	16.3	3.0	16.0	2.8	2.0	0.4	34.5	4.1
130	16.0	3.0	17.4	3.0	1.9	0.4	35.3	4.3
100	16.3	3.0	16.6	3.0	1.9	0.4	34.8	4.3
80	17.0	3.0	18.1	3.0	2.1	0.5	37.2	4.3
60	20.0	3.2	23.0	3.2	2.1	0.5	45.1	5.0
48	20.1	3.3	25.7	3.3	2.2	0.5	47.9	5.5
$\Delta\sigma_{\text{absolute}}$		22%		17%		20%		20%

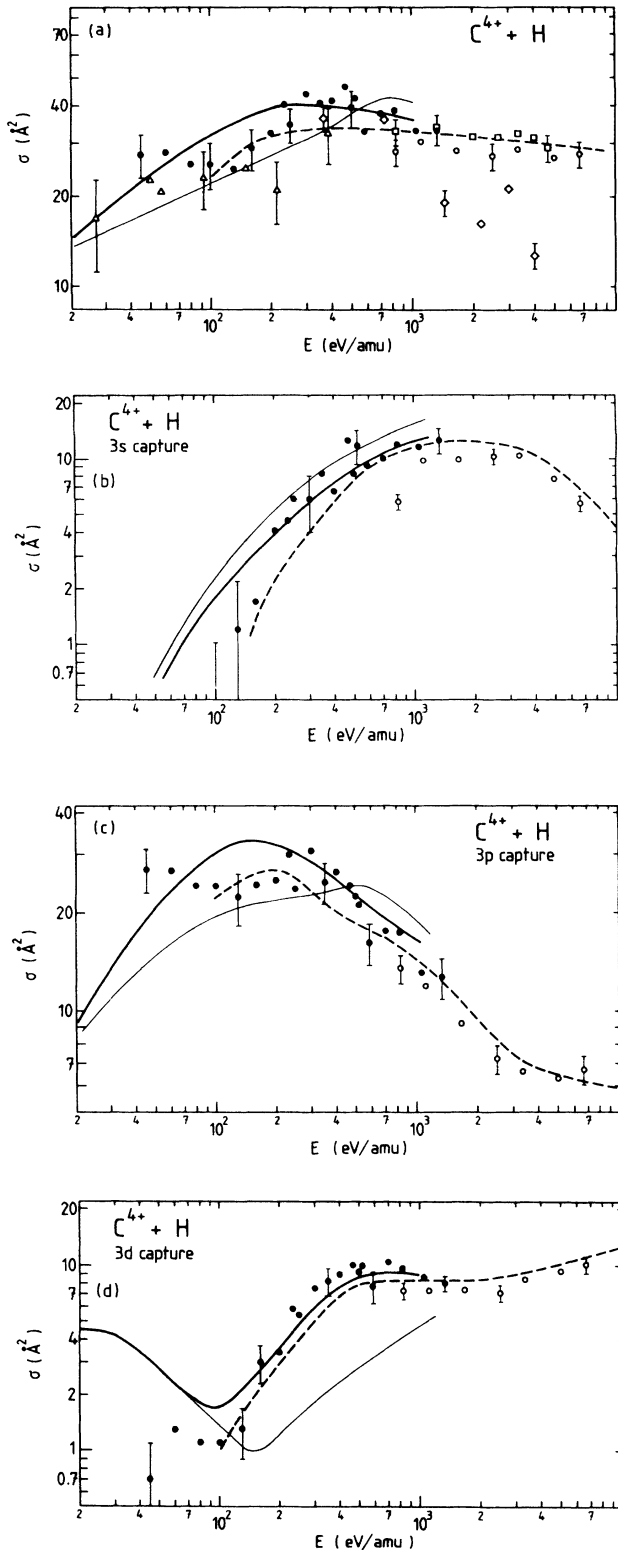


FIG. 4. State selective and total electron-capture cross sections for C^{4+} colliding with atomic hydrogen. Theory: thick solid line, MO7, Gargaud *et al.* (Ref. 10); thin solid line, MO4, Gargaud and McCarroll, (Ref. 17); dashed line, AO+, Fritsch and Lin (Ref. 16). Charge-changing experiments: squares, Dijkkamp *et al.* (Ref. 11); diamonds, Panov *et al.* (Ref. 33); triangles, Phaneuf *et al.* (Ref. 6). Photon-emission experiments: open circles, Dijkkamp *et al.* (Ref. 11); closed circles, this work.

only show up as tiny peaks in our spectra (see Fig. 3) have larger branching ratios than the $4l \rightarrow 3l'$ transitions (a factor of ~ 1.5 for $4s$ and a factor of ~ 3 for $4p$ and $4d$).³⁰ So because of the smallness of the $4l \rightarrow 2l'$ transitions compared to the $3l \rightarrow 2l'$ transitions ($< 5\%$) it is justified to neglect the contribution of the $4s$, $4p$, and $4d$ states to the $3l$ population. Since the wavelength of the $4f \rightarrow 3d$ lies outside the spectral range of the monochromators it was not possible to check this cascade contribution to the $3d$ states. However, from the measurements of Dijkkamp *et al.*¹¹ it is to be expected that also this contribution is certainly much smaller than 5%. Nevertheless, we included for all $3l$ states an error of 5% due to cascades.

The absolute systematic error in the state-selective cross section ranges from 17% to 22%, see Tables I and II. Especially in the case of atomic hydrogen these systematic errors are smaller than in previous work.^{11,12} This is due to the fact that the CIV $3p \rightarrow 2s$ transition at 31.2 nm is close to a calibration point for the monochromator, namely the HeII $2p \rightarrow 1s$ transition at 30.4 nm. The sensitivity at this wavelength has been determined by using the accurately measured HeII $2p \rightarrow 1s$ emission cross sections for He^{2+} impact on atomic hydrogen (error 15%).²⁹ Therefore we have taken the absolute systematic error in the $3p \rightarrow 2s$ emission cross section to be the quadratic sum of the previous He^{2+} measurements (15%) and the statistical error in the calibration measurement. The errors in the $3d \rightarrow 2p$ (38.4 nm) and the $3s \rightarrow 2p$ (42.0 nm) transitions include an extra error of, respectively, 8% and 12% due to uncertainties in the wavelength-dependent sensitivity of the spectrometer.

With respect to the systematic error we still have to consider the role of metastable projectile ions. There are no $C^{4+} (1s2s)^1S$ ions in the beam since their lifetime of $\sim 3 \mu s$ (Ref. 31) is much shorter than the $\sim 11 \mu s$ needed for the transport of the 16 keV C^{4+} beam from the ECR ion source to the setup. However the $C^{4+} (1s2s)^3S$ survive the transport and from Auger electron measurements—after a time of flight of 14 μs —the metastable fraction was found to be $5 \pm 2\%$.³² The metastables themselves do not interfere with the photon-emission measurements, because of the fact that electron capture leads to doubly excited states which autoionize. However, the uncertainty in the fraction of metastables introduces a systematic error of 2% in the fraction of ground-state ions, since the ground-state fraction is $95 \pm 2\%$.

IV. DISCUSSION

A. General classical considerations

Before making a detailed comparison between experimental results (Figs. 4 and 5) and quantal calculations it is instructive to compare general tendencies with the “dynamic” version (Niehaus³⁴) of the classical over-barrier model. With this model we have calculated the reaction windows for electron capture in collisions of 250 eV/amu C^{4+} with atomic and molecular hydrogen. Figure 6 shows the reaction windows together with the $3l$ energy

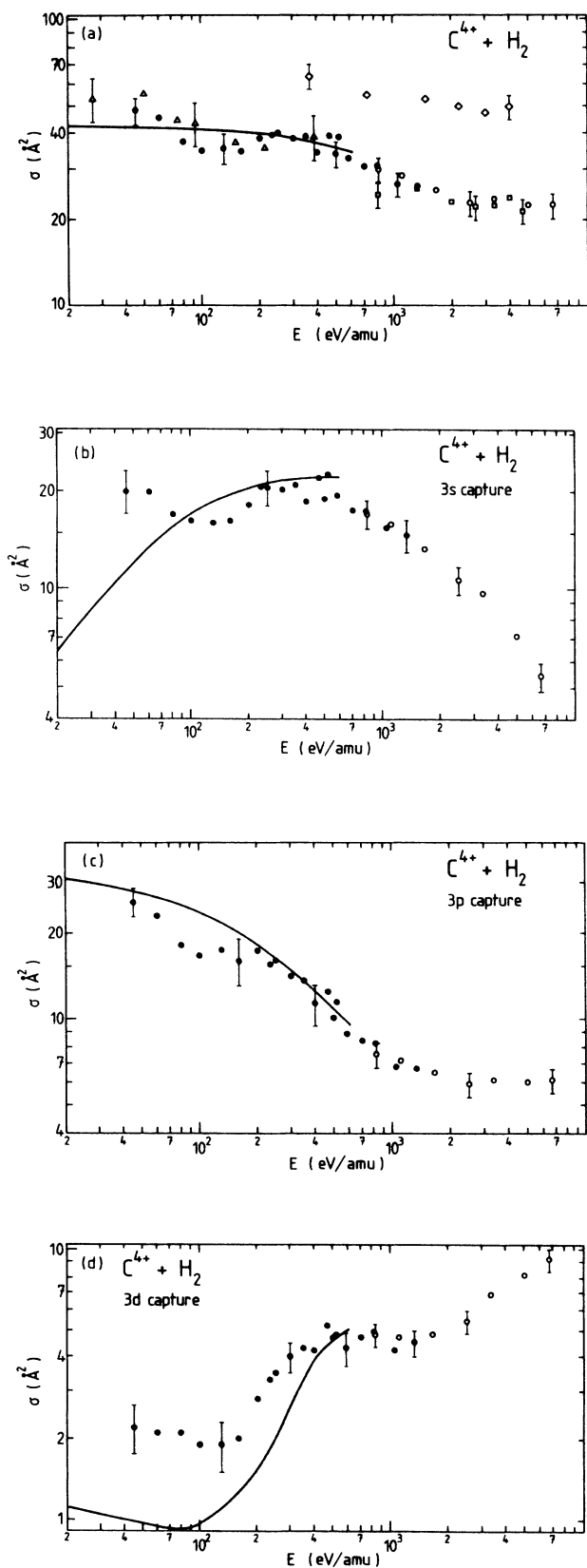


FIG. 5. State-selective and total electron-capture cross sections for C^{4+} colliding with molecular hydrogen. Theory: solid line, Gargaud and McCarroll (Ref. 17). Experiment: as in Figs. 4(a)–4(d).

levels in C^{3+} . From Fig. 6 it can be seen that whereas the $3l$ levels are favorably situated in the H_2 reaction window they are on the edge of the H reaction window. The $4l$ levels lie around 14 eV and hence it is clear that the $4l$ states are only weakly populated in collisions of C^{4+} with atomic and molecular hydrogen. From the favorable position of the $3l$ states in the case of H_2 it is to be expected that the total electron-capture cross section, σ_i is larger for collision on H_2 than on H . Comparing Figs. 4(a) and 5(a) it is found that below 250 eV/amu $\sigma_i(H_2) > \sigma_i(H)$ and that at higher impact energies $\sigma_i(H_2) \cong \sigma_i(H)$. That the difference between H and H_2 is not that pronounced may be understood from the following facts. (i) σ_i is proportional to the square of the internuclear distance,³⁴ R_{CB} , at which the potential barrier between ion and target becomes low enough for the target electron to be transferred to the ion [to cross the classical barrier (CB)]. R_{CB} is 5.3 and 4.4 a.u. for H and H_2 , respectively. (ii) The width of the reaction window³⁴ changes proportional to $v^{1/2}$ (v is the velocity of the C^{4+} ions) and hence at higher energies the window widens so that the actual positions of the energy levels become less important.

To some extent even the state-selective cross sections, $\sigma(3l)$ can be explained in the picture of the classical model. From the positions in the H reaction window we expect $\sigma(3s)$ to be relatively small and $\sigma(3p)$ and $\sigma(3d)$ to be of the same order of magnitude. Whereas the first expectation is confirmed by the experiments the latter one is not since $\sigma(3p)$ turns out to be much larger than $\sigma(3d)$ [see Figs. 4(b)–4(d)]. This can be understood from angular momentum arguments,³⁵ namely in the frame of the C^{4+} ion, the target electron has an apparent angular momentum of the order of bv with b the impact parameter. For collisions on H the maximum value of b , R_{cb} is 5.3 a.u. therefore the angular momentum for 250 eV/amu C^{4+} ($v = 0.1$ a.u.) ranges between 0 and 0.53. These values fit obviously better to the p than to the d state. Considering the positions of the $3l$ levels in the reaction window and the angular momentum argument, $\sigma(3p)$ and $\sigma(3s)$ are expected to be of the same order of magnitude and both much larger than $\sigma(3d)$ in the case of collisions on molecular hydrogen. This is indeed so, see Figs. 5(b)–5(d). Whereas some main features of the electron-

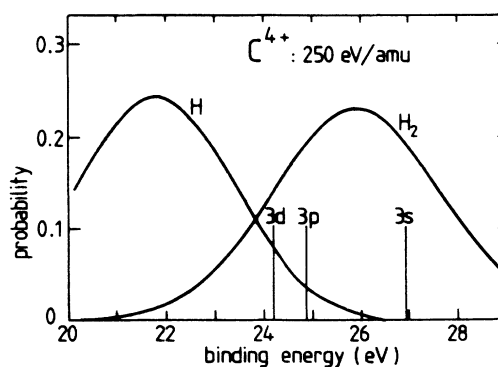


FIG. 6. Reaction windows for electron capture in collisions of 250-eV/amu C^{4+} with atomic and molecular hydrogen.

capture processes can be understood from classical considerations fully quantal calculations are needed to describe the finer details.

B. Collisions on atomic hydrogen

In Figs. 4(a)–4(d) the measured state-selective, $\sigma(3l)$, and total, $\sigma_i = \sum_l \sigma(3l)$, electron-capture cross sections are compared with the results of the three calculations, that presented not only σ_i but also $\sigma(3l)$.^{10,16,17} The two calculations, by Gargaud *et al.*¹⁰ (MO7) and Gargaud and McCarroll¹⁷ (MO4), which use molecular orbitals as basis set are essentially the same, they only differ in the number of molecular states included. The older calculations, MO4 include only the σ orbitals correlated to the $n = 3$ manifold of C IV, the more recent calculations MO7 include also the π and δ orbitals. Hence MO7 includes both radial and rotational coupling whereas MO4 only includes radial coupling. The AO+ calculations by Fritsch and Lin¹⁶ use atomic orbitals, namely all $n = 3, 4$, and 5 C IV orbitals, the H(1s) orbital and some united atom orbitals to account for molecular binding effects at the lower velocities.

As seen from Fig. 4(a), which shows the results for total charge transfer the present results are a logical extension to lower energies of the optical and charge changing measurements by Dijkkamp *et al.*¹¹ Furthermore, they are in good agreement with the charge changing measurements by Phaneuf *et al.*,⁶ although the dip at 200 eV/amu seen by Phaneuf *et al.*⁶ is not present in our results which change more smoothly with energy. Nevertheless our measurements confirm the discrepancy in the energy range of 80 to 200 eV/amu between experiment and MO7. The results of MO7 are supported by theoretical work of Olson *et al.*¹⁴ and Hanssen *et al.*¹⁵

From the state-selective cross sections shown in Figs. 4(b)–4(d) it can be seen that there is generally a fair agreement between experiment and theory. However, some important deviations with respect to the state-selective electron-capture cross sections should be noted: (i) Below 200 eV/amu $\sigma(3s)$ decreases more rapidly with decreasing energy than the MO4 and MO7 results. (ii) in the energy range below 400 eV/amu $3p$ is by far the most dominantly populated state with a more or less constant cross section. Therefore the difference between experiment and MO7 for $\sigma(3p)$ is the reason for the difference observed in comparing the total charge transfer cross sections. (iii) in our results we do not observe the increase in $\sigma(3d)$ at the lowest results, predicted by MO7 and MO4. Furthermore, in the energy of 100–1000 eV/amu the MO4 results underestimate $\sigma(3d)$ by a factor of 2. Together with the discrepancies for $\sigma(3s)$ and $\sigma(3p)$ it may be concluded that the agreement between the measured σ_i and the MO4 results is to some extent fortuitous. Except for some small differences between 200 and 450 eV/amu the AO+ results are in good agreement with the experiments over two decades of energy (0.1–10 keV/amu).

Differences become more clear from the *relative* populations of the $3l$ states, $\sigma_{rel}(3l) = \sigma(3l) / \sum_l \sigma(3l)$ since in

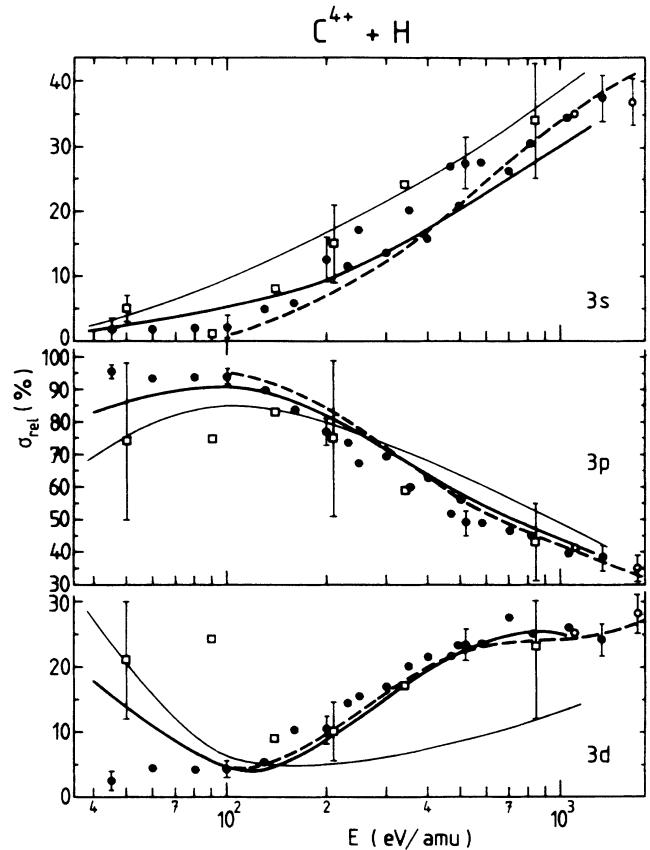


FIG. 7. Relative state-selective electron-capture cross sections, $\sigma(3l)/\sum_l \sigma(3l)$ for C^{4+} colliding with atomic hydrogen. Theory: thick solid line, Gargaud *et al.* (Ref. 10); thin solid line, Gargaud and McCarroll (Ref. 17); dashed line, Fritsch and Lin (Ref. 16). Experiments: open squares, Baptist *et al.* (Ref. 33); open circles, Dijkkamp *et al.* (Ref. 11); closed circles, this work.

that way we remove the largest contribution to the scatter in $\sigma(3l)$, namely the overlap of ion and target beams (see section on experimental results). The $\sigma_{rel}(3l)$ are shown in Fig. 7 together with the AO+, MO7, and MO4 predictions and the experimental results of Dijkkamp *et al.*¹¹ and Baptist *et al.*³³ For energies above 100 eV/amu there is good agreement between experiments and MO7 and AO+ calculations. The MO4 results are at variance with the experiments which indicates the importance of rotational couplings which have not been included in the MO4 calculation. In that respect it should be noted that whereas in the energy range of 100 to 200 eV/amu the results of the MO7 work differ in absolute value [see Figs. 4(a)–4(d)], the $\sigma_{rel}(3l)$ are in good agreement with experiment. Below 100 eV/amu the theory predicts a decrease in $\sigma_{rel}(3p)$ and a strong increase in $\sigma_{rel}(3d)$. This effect is not yet observed in our measurements which are therefore also in disagreement with the results of Baptist *et al.*³³ The reason for this discrepancy is yet unclear, however, with different lens settings we could reproduce the results at 60 eV/amu within error bars. In conclusion it may be stated that

below 100 eV/amu the total charge-transfer cross sections are in agreement with the MO7 calculations however the l distribution is clearly different.

C. Collisions on molecular hydrogen

The state selective, $\sigma(3l)$, total, $\sigma_t = \sum_l \sigma(3l)$, and relative, $\sigma_{\text{rel}}(3l)$, electron-capture cross sections are shown in Figs. 5(a)–5(d) and 8. In the case of collisions on molecular hydrogen theoretical work is restricted to the calculations of Gargaud and McCarroll¹⁷ which include only the σ orbitals. Just as for collisions on atomic hydrogen we note that the theoretical and experimental total cross sections are in fair agreement with each other, whereas especially below 100 eV/amu the l distributions differ. Our results can be seen to agree with the optical measurements by Dijkkamp *et al.*¹¹ and the charge-changing measurements by Phaneuf *et al.*⁵ and Dijkkamp *et al.*¹¹ It is not obvious that the summed emission cross sections can be compared with the results of charge-changing measurements since the latter include contributions from double electron capture followed by

autoionization. At energies of a few keV/amu cross sections for autoionizing double capture are smaller than $3 \times 10^{-16} \text{ cm}^2$.^{32,36–38} Since furthermore the reaction channels leading to double electron capture into autoionizing states lie outside the reaction window for double electron capture³² it is certainly not to be expected that the cross sections will increase with lowering the impact energies. Hence the effect of double electron capture followed by autoionization on the charge-changing cross sections is small.

Inspecting the relative cross sections shown in Fig. 8 it is seen that above 100 eV/amu there is good agreement between experiment and theory. This is somewhat unexpected since in the case of atomic hydrogen the calculations without rotational coupling did differ from experiment. This may indicate that for collisions of C^{4+} on molecular hydrogen rotational couplings are not that important, in contrast to the case of collisions on atomic hydrogen. Together with the fact that below 100 eV/amu there are discrepancies, this certainly indicates the need for some new theoretical investigations of electron capture in collisions with molecular hydrogen.

V. CONCLUSION

It has been shown that it is possible to decelerate C^{4+} beams of 1.33 keV/amu down to 0.05 keV/amu by means of a five-element electrostatic lens system and to perform photon-emission spectroscopy measurements. The measurements on C^{4+} -H collisions show that the long-standing discrepancy in the energy range of 100 and 200 eV/amu between total charge-transfer measurements and calculations based on molecular state expansions^{10,14,15} is real and mainly due to differences in the cross sections for electron capture into the $3p$ state. Furthermore it has been shown that for energies below 100 eV/amu the theoretical^{10,17} and experimental l distributions are not in accordance with each other which is also seen for the case of collisions with molecular hydrogen. Furthermore, our measurements seem to indicate that for C^{4+} -H rotational couplings are important whereas for C^{4+} -H₂ they may be not that important to get the correct l distribution in the energy range of 100 to 1000 eV/amu. These differences make an improvement in the theoretical description desirable, especially since also the result of a general analytical model by Abramov *et al.*,³⁹ developed to predict the l distribution in collisions of fully stripped ions and atomic hydrogen, seems not to be applicable to C^{4+} -H collisions. An extended version of this model (Janev and Winter¹) includes both radial and rotational coupling and yields an l distribution peaking at $l=2$ which is not observed in the experiments.

ACKNOWLEDGMENTS

The authors would like to thank J. Eilander and J. Sijbring for their excellent technical support. This work is part of the research program and the Stichting voor Fundamenteel Onderzoek der Materie (FOM) with financial support by the Stichting voor Nederlands Wetenschappelijk Onderzoek (NWO).

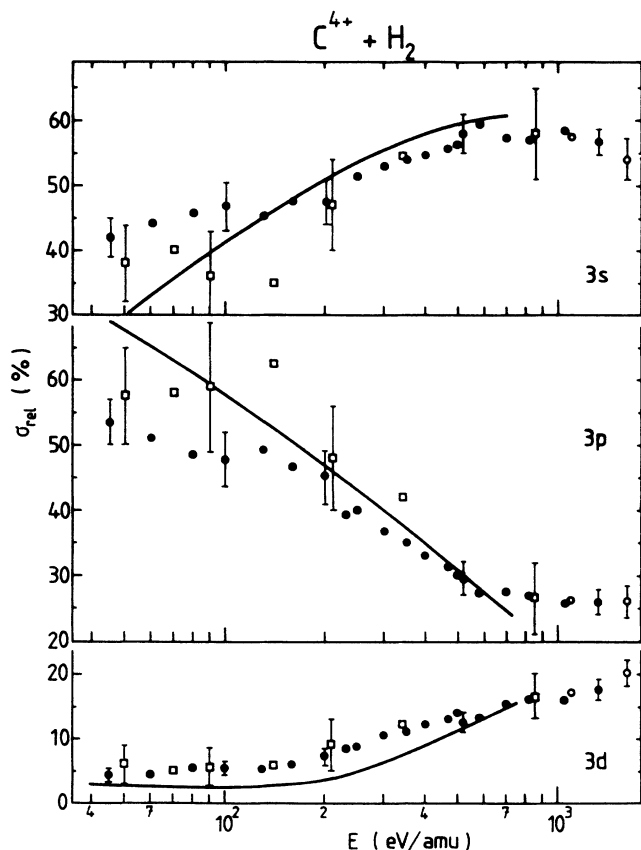


FIG. 8. Relative state-selective electron-capture cross sections, $\sigma(3l)/\sum_l \sigma(3l)$ for C^{4+} colliding with molecular hydrogen. Theory: solid line, Gargaud and McCarroll (Ref. 17); Experiments: open squares, Baptist *et al.* (Ref. 33); open circles, Dijkkamp *et al.* (Ref. 11); closed circles, this work.

*Permanent address: FOM–Institute for Atomic and Molecular Physics, P.O. Box 41883, 1009 DB Amsterdam, The Netherlands.

- ¹R. K. Janev and H. Winter, *Phys. Rep.* **117**, 265 (1985).
- ²H. B. Gilbody, *Adv. At. Mol. Phys.* **22**, 143 (1986).
- ³T. G. Heil, *Nucl. Instrum. Methods B* **23**, 222 (1987).
- ⁴R. J. Fonck, D. S. Darrow, and K. P. Jähnig, *Phys. Rev. A* **29**, 3288 (1984).
- ⁵A. Boileau, M. von Hellerman, L. D. Horton, J. Spence, and H. P. Summers, *Plasma Phys. Controlled Fusion* **31**, 779 (1989).
- ⁶R. A. Phaneuf, I. Alvarez, F. W. Meyer, and D. H. Crandall, *Phys. Rev. A* **26**, 1892 (1982).
- ⁷C. C. Havener, M. S. Huq, H. F. Krause, P. A. Schulz, and R. A. Phaneuf, *Phys. Rev. A* **39**, 1725 (1989).
- ⁸M. S. Huq, C. C. Havener, and R. A. Phaneuf, *Phys. Rev. A* **40**, 1811 (1989).
- ⁹M. Gargaud and R. McCarroll, *J. Phys. B* **21**, 513 (1988).
- ¹⁰M. Gargaud, R. McCarroll, and P. Valiron, *J. Phys. B* **20**, 1555 (1987).
- ¹¹D. Dijkkamp, D. Čirič, E. Vlieg, A. de Boer, and F. J. de Heer, *J. Phys. B* **18**, 4763 (1985).
- ¹²R. Hoekstra, D. Čirič, F. J. de Heer, and R. Morgenstern, *Phys. Scr.* **T28**, 81 (1989).
- ¹³R. Hoekstra, A. R. Schlatmann, F. J. de Heer, and R. Morgenstern, *J. Phys. B* **22**, L603 (1989).
- ¹⁴R. E. Olson, E. J. Shipsey, and J. C. Browne, *J. Phys. B* **11**, 699 (1978).
- ¹⁵J. Hanssen, R. Gayet, C. Harel, and A. Salin, *J. Phys. B* **17**, L323 (1984).
- ¹⁶W. Fritsch and C. D. Lin, *J. Phys. B* **17**, 3271 (1984).
- ¹⁷M. Gargaud and R. McCarroll, *J. Phys. B* **18**, 463 (1985).
- ¹⁸R. Geller and B. Jacquot, *Nucl. Instrum. Methods* **202**, 399 (1982).
- ¹⁹A. G. Drentje, *Nucl. Instrum. Methods B* **9**, 526 (1985).
- ²⁰M. Menzinger and R. Wolfgang, *J. Chem. Phys.* **50**, 2991 (1969).
- ²¹L. Folkerts (private communication).
- ²²S. T. de Zwart, Ph.D. thesis, R. U. Gronigen, 1987.
- ²³M. Fehring, M. Delaunay, R. Geller, P. Varga, and H. Winter, *Nucl. Instrum. Methods B* **23**, 245 (1987).
- ²⁴J. Slevin and W. Stirling, *Rev. Sci. Instrum.* **52**, 1780 (1981).
- ²⁵D. Čirič, D. Dijkkamp, E. Vlieg, and F. J. De Heer, *J. Phys. B* **18**, 4745 (1985).
- ²⁶P. N. Clout and D. W. O. Heddle, *J. Opt. Soc. Am.* **59**, 715 (1969).
- ²⁷R. Hoekstra, M. G. Suraud, F. J. de Heer, and R. Morgenstern, *J. Phys. (Paris) Colloq.* **50**, 387 (1989).
- ²⁸K. Kadota, D. Dijkkamp, R. L. van der Woude, A. de Boer, G. Y. Pan, and F. J. De Heer, *J. Phys. B* **15**, 3275 (1982).
- ²⁹R. Hoekstra, F. J. de Heer, R. Morgenstern, and W. Fritsch (unpublished).
- ³⁰J. Z. Klose and W. L. Wiese, *J. Quant. Spectrosc. Radiat. Transfer* **42**, 337 (1989).
- ³¹G. W. F. Drake, G. A. Victor, and A. Dalgarno, *Phys. Rev.* **180**, 25 (1969).
- ³²E. M. Mack, Ph.D. thesis, R. U. Utrecht, 1987.
- ³³R. Baptist, J. J. Bonnet, M. Bonnefoy, E. Boursey, A. Brenac, M. Chassevent, G. Chauvet, S. Dousson, Y. Le Duff, A. Fleury, M. Gargaud, and D. Hitz, *Nucl. Instrum. Methods B* **23**, 123 (1987).
- ³⁴A. Niehaus, *J. Phys. B* **19**, 2925 (1986).
- ³⁵J. Burgdörfer, R. Morgenstern, and A. Niehaus, *Nucl. Instrum. Methods B* **23**, 120 (1987).
- ³⁶A. Bordenave-Montesquieu, M. Boudjema, P. Benoit-Cattin, A. Gleizes, and P. Moretto-Capelle, *J. Phys. (Paris) Colloq.* **50**, 305 (1989).
- ³⁷N. Stolterfoht, C. C. Havener, R. A. Phaneuf, J. K. Swenson, S. M. Shafroth, and F. W. Meyer, *Phys. Rev. Lett.* **57**, 74 (1986).
- ³⁸R. Mann and H. Schulte, *Z. Phys. D* **4**, 343 (1987).
- ³⁹V. A. Abramov, F. F. Baryshnikov, and V. S. Lisita, *JETP Lett.* **27**, 464 (1978).